

# Stability Analysis of Coupled Map Lattices at Locally Unstable Fixed Points

Harald Atmanspacher<sup>1,2</sup>, Thomas Filk<sup>2,3</sup>, and Herbert Scheingraber<sup>1</sup>

1 Center for Interdisciplinary Plasma Science,  
Max-Planck-Institut für extraterrestrische Physik,  
85740 Garching, Germany

2 Department of Theory and Data Analysis,  
Institute for Frontier Areas of Psychology and Mental Health,  
Wilhelmstr. 3a, 79098 Freiburg, Germany

3 Institute of Physics, University of Freiburg,  
Hermann-Herder-Str. 3, 79104 Freiburg, Germany

Accepted for publication in *European Physical Journal B*

PACS: 05.45.Ra, 05.45.Xt, 89.75 Hc

## Abstract

Numerical simulations of coupled map lattices (CMLs) and other complex model systems show an enormous phenomenological variety that is difficult to classify and understand. It is therefore desirable to establish analytical tools for exploring fundamental features of CMLs, such as their stability properties. Since CMLs can be considered as graphs, we apply methods of spectral graph theory to analyze their stability at locally unstable fixed points for different updating rules, different coupling scenarios, and different types of neighborhoods. Numerical studies are found to be in excellent agreement with our theoretical results.

# 1 Introduction

Coupled map lattices (CMLs) are arrays of cells whose state value is continuous, usually within the unit interval, over discrete space and time. Starting with Turing's seminal work on morphogenesis [1], they have been used to study the behavior of complex spatiotemporal systems for more than 50 years. More recently, Kaneko and collaborators have established many interesting results for CMLs [2] as generalizations of cellular automata, whose state values are discrete.

One key motivation for modeling spatiotemporally extended systems with CMLs is to simplify the standard approach in terms of partial differential equations. And, of course, CMLs would not have become accessible without the rapid development of fast computers with large storage capacities. Within the last decades, CMLs have been applied to the study of areas as diverse as social systems, ecosystems, neural networks, spin lattices, Josephson junctions, multimode lasers, hydrodynamical turbulence, and others (cf. the special journal issues *CHAOS* **2**(3), 1992, and *Physica D* **103**, 1997).

A compact characterization of a CML with one time parameter is given by

$$u(n+1, x) = (1 - \epsilon)f(u(n, x)) + \frac{\epsilon}{n_x} \sum_{y \sim x} g(u(n, y)) , \quad (1)$$

where  $x$  represents the sites of the lattice,  $x = 1, \dots, N_{tot}$ , here considered as the vertices of a graph, and  $n$  represents the time step of the iteration. The parameter  $\epsilon$  specifies the coupling between each cell and its neighborhood (and is often considered as constant over time and space). The sum over  $y \sim x$  is the sum over all  $n_x$  neighbors  $y$  of vertex  $x$ . The function  $g$  characterizes the interaction of a vertex with its neighborhood and will be explained below.

As in many other studies of CMLs,  $f(x)$  is the logistic map on the unit interval,

$$f(x) = rx(1 - x) ,$$

with  $0 \leq r \leq 4$ . For  $r \geq 1$  the logistic map has a critical point at  $\frac{r-1}{r}$  which is unstable for  $3 < r \leq 4$ . The relevance of maps with quadratic maximum (such as the logistic map) for models of neurobiological networks was recently substantiated by novel results concerning a non-monotonic (rather than sigmoid) transfer function for individual neurons [3].

For  $\epsilon \rightarrow 0$ , there is no coupling at all; hence, local neighborhoods have no influence on the behavior of the CML. This situation represents the limiting case of  $N_{tot}$  independently operating local objects at each lattice site. In the general case  $0 < \epsilon < 1$ , the independence of individual cells is lost and the lattice behavior is governed by both local and global influences, depending on the chosen neighborhood. CMLs with a maximal neighborhood,  $n_x \approx N_{tot}$ , are often denoted as globally coupled maps. Their behavior is determined by global properties alone (mean field approach).

The function

$$g(x) = \alpha x + \beta f(x) + \gamma f(f(x)) , \quad (2)$$

with

$$\alpha + \beta + \gamma = 1 \quad \alpha, \beta, \gamma \geq 0 ,$$

allows us to treat the interaction between each vertex and its neighborhood in different ways, depending on its time scale  $\Delta t$ . If the interaction can be regarded as simultaneous,  $\Delta t \approx 0$ , the situation can be approximated by  $\alpha = \gamma = 0$  and  $\beta = 1$ . Such a type of coupling, sometimes called “future coupling” [4], will be referred to as *non-causal coupling* [5] in the following, since the simultaneity of the interaction between vertex and neighbors makes a clear distinction of cause and effect impossible.

The situation of a finite interaction time  $\Delta t > 0$  can be properly modeled by  $\beta = \gamma = 0$  and  $\alpha = 1$ . In this way, past states in the neighborhood of a vertex are considered to act on the present state of the vertex with limited signal speed, so that the effect of an interaction is delayed with respect to its cause. Such a type of coupling will therefore be denoted as *causal coupling* in the following. Corresponding lattice behavior has recently been studied in [4, 6, 7, 8, 9].

A third, somewhat exotic possibility arises for  $\alpha = \beta = 0$  and  $\gamma = 1$ . This case reflects the idea to model the action of future states of a vertex neighborhood on a present vertex state. More precisely, this refers to *locally extrapolated* future states and is justified for small  $\epsilon$  since then  $u(n+1, y) \approx f(u(n, y))$ . In this interpretation, the case of non-vanishing  $\gamma$  is in contradiction with causality; thus we refer to such a situation as *anti-causal coupling*.

The inclusion of anti-causal coupling can be interesting if one wants to study the consequences of a decomposition of a fundamental time-reversal invariant evolution of a system into forward and backward components. Using such a decomposition, one can investigate the influence of both components on the stability properties of CMLs. It has indeed been found that the stability of CMLs is supported by large  $\alpha$ , and their stability is obstructed if  $\alpha$  is small [5]. Based on these observations, one may speculate that stability acts as a selection criterion for a forward arrow of time [10].

Another time scale important for the physical interpretation of eq. (1) is the time interval  $\Delta\tau$  assumed for the updating mechanism, i.e. for the physical integration of signals from the neighborhood states with the vertex state considered. If signals between vertices are transmitted much slower than the time scale assumed for the updating mechanism,  $\Delta\tau \ll \Delta t$ , the updating can be implemented (almost) instantaneously, or *synchronously*. If this is not the case,  $\Delta\tau \gtrsim \Delta t$ , updating must be implemented *asynchronously*. This entails the additional problem of determining a proper updating sequence, which can be random or depend on particular features of the situation considered.

Most of the work on CMLs published in this respect (cf. [11]) was based on synchronous updating. For asynchronous updating as, for instance, studied by Lumer & Nicolis [12], it was found that the behavior of CMLs differs strongly from that of CMLs with synchronous updating. Additional results for asynchronous updating were reported by [13, 14, 4, 5, 9]. Asynchronous updating rules have been suggested as particularly relevant for neurobiological networks.

As a common feature of the (so far) few studies of asynchronous updating, it has been reported that it facilitates the synchronization and stabilization of CMLs decisively. In particular, Mehta & Sinha [4] demonstrated that the dynamics at individual lattice cells is strongly synchronized by coupling among cells. Atmanspacher & Scheingraber [5, 9] showed that unstable fixed points at individual vertices can be stabilized as a consequence of their coupling to neighboring unstable fixed points.

Such a stabilization is of particular interest since it is independent of external control mechanisms. The global stabilization of unstable local behavior operates inherently, without external adjustment, once the coupling is strong enough. Such a possibility represents a powerful alternative to external control procedures in the style of “controlling chaos” [15].

Most published results concerning the stabilization and synchronization of CMLs have been obtained by numerical studies for various parameters due to different coupling, different neighborhoods, and different updating. A number of theoretical approaches have been developed to describe these numerical results analytically [16, 17, 18, 19, 20]. In this contribution we present, for the first time, a comprehensive stability analysis of CMLs at locally unstable fixed points, which allows us to understand corresponding numerical results theoretically. In particular, the sophisticated dependence of the stabilization behavior on the different parameters mentioned above [5, 9] can be clarified.

As recently proposed by Jost & Joy [21] and by Belykh et al. [22], the stability properties of CMLs can be compactly and conveniently analyzed in a graph theoretical manner. We first determine, in section 2, the eigenvalues of the adjacency matrices related to various neighborhoods on regular lattices. In section 3, we derive a stability condition for synchronous update and constant solutions of the logistic map and apply it to special cases for causal and non-causal coupling numerically studied in [5, 9]. In addition, theoretical and numerical results are obtained for the situation of anti-causal coupling. In all cases, the agreement between theoretical and numerical results is excellent. In section 4, we present an intuitive argument for a stability analysis with asynchronous update. In section 5, the discussion is extended to generalized neighborhoods. Section 6 summarizes and concludes the paper, and some perspectives are addressed.

## 2 The Spectrum of a Graph

A CML can be considered within the more general framework of the theory of graphs, whose properties can be studied by well-developed analytic methods [23, 24]. A graph is defined by a set  $F$  of vertices, a set  $E$  of edges, and a map  $\delta^\pm : E \rightarrow F$  indicating whether a vertex is an initial point or a terminal point for an edge. A CML can be implemented on a graph with no self-loops, no multiple edges, and only undirected edges. Such graphs are sometimes referred to as *simple* graphs (cf. [25]). Many interesting properties of CMLs, in particular their stability properties, can then be investigated by two basic matrices characterizing the corresponding graph:

its *adjacency matrix* and its *valence matrix*.

For an arbitrary simple graph (defined by the “neighbor-relation”  $\sim$  between its vertices), the adjacency matrix  $A(x, y)$  and the valence matrix  $V(x, y)$  are defined by:

$$A(x, y) = \begin{cases} 1 & \text{for } y \sim x \\ 0 & \text{otherwise} \end{cases}$$

and

$$V(x, y) = \begin{cases} n_x & \text{for } x = y \\ 0 & \text{otherwise} \end{cases} \quad \text{with } n_x = \sum_y A(x, y),$$

where  $n_x$  is the number of neighbors of vertex  $x$ . The matrix  $A$  contains only 1s and 0s (no multiple edges), is non-reflexive (zero diagonal since there are no self-loops) and symmetric (undirected edges). If the valence matrix is proportional to the identity matrix,  $V = v \mathbf{1}$ , the graph is called *regular*.

For the eigenvalues  $\lambda$  of  $V^{-1}A$  we have  $|\lambda| \leq 1$  since  $V^{-1}A$  is a Markov matrix, i.e.  $(V^{-1}A)_{ij} \geq 0$  and  $\sum_j (V^{-1}A)_{ij} = 1$ . The eigenvalue  $\lambda_{\max} = +1$  is assumed for the constant vector  $u(x)$ . However, we will see that the lower bound for the eigenvalues of  $V^{-1}A$  can deviate remarkably from  $-1$ . From  $\text{tr } V^{-1}A = 0$  we can only deduce that the lower bound has to be negative (for infinite graphs it can be zero).

In the following, we consider regular graphs,  $V = v \mathbf{1}$ . We determine the eigenvalues for the adjacency matrix for different types of neighborhoods on a 2-dimensional  $N \times N$  square lattice with periodic boundary conditions. In particular, we focus on the following types of neighborhoods: von Neumann 1st order (the four nearest neighbors horizontally and vertically), Moore 1st order (the eight nearest neighbors including the diagonal neighbors), von Neumann 2nd order (Moore 1st order plus the next to nearest neighbors horizontally and vertically), and Moore 2nd order (the 24 lattice sites in a  $5 \times 5$  square around the central point).

The eigenvalues are calculated by introducing the shift matrix:

$$P = \begin{pmatrix} 0 & 1 & 0 & 0 & 0 & \cdots & 0 \\ 0 & 0 & 1 & 0 & 0 & \cdots & 0 \\ \vdots & \vdots & \vdots & \vdots & \vdots & \vdots & \\ 0 & 0 & 0 & 0 & 0 & \cdots & 1 \\ 1 & 0 & 0 & 0 & 0 & \cdots & 0 \end{pmatrix}.$$

$P$  is a unitary matrix with  $P^N = \mathbf{1}$  and  $P^{-1} = P^+ = P^{N-1}$ . Therefore, the eigenvalues  $\omega_k$  of  $P$  satisfy  $\omega_k^N = 1$  and are given by the  $N$  square roots of 1:

$$\omega_k = \exp(i\phi) = \exp\left(\frac{2\pi ik}{N}\right) \quad \text{with } k = 0, 1, \dots, N-1.$$

On a 2-dimensional  $N \times N$  lattice we define the two shift operators for each direction by:

$$P_1 = P \otimes \mathbf{1} \quad \text{and} \quad P_2 = \mathbf{1} \otimes P.$$

The adjacency matrices for the different neighborhoods commute with  $P_1$  and  $P_2$  and can be completely expressed in terms of these operators:

$$\begin{aligned}
A_{v.N.1} &= P_1 + P_1^{-1} + P_2 + P_2^{-1} \\
A_{M.1} &= (\mathbf{1} + P_1 + P_1^{-1})(\mathbf{1} + P_2 + P_2^{-1}) - \mathbf{1} \\
A_{v.N.2} &= (\mathbf{1} + P_1 + P_1^{-1})(\mathbf{1} + P_2 + P_2^{-1}) - \mathbf{1} + P_1^2 + P_1^{-2} + P_2^2 + P_2^{-2} \\
A_{M.2} &= (\mathbf{1} + P_1 + P_1^{-1} + P_1^2 + P_1^{-2})(\mathbf{1} + P_2 + P_2^{-1} + P_2^2 + P_2^{-2}) - \mathbf{1} .
\end{aligned}$$

Therefore, the eigenvalues of  $A$  are given by:

$$\begin{aligned}
v.N.1 : \quad & 2 \cos \phi_1 + 2 \cos \phi_2 \\
& \text{with } \phi_i = \frac{2\pi k_i}{N} \text{ where } k_i = 0, 1, \dots, N-1 . \\
M.1 : \quad & (1 + 2 \cos \phi_1)(1 + 2 \cos \phi_2) - 1 \\
v.N.2 : \quad & (1 + 2 \cos \phi_1)(1 + 2 \cos \phi_2) - 1 + 2 \cos 2\phi_1 + 2 \cos 2\phi_2 \\
M.2 : \quad & (1 + 2 \cos \phi_1 + 2 \cos 2\phi_1)(1 + 2 \cos \phi_2 + 2 \cos 2\phi_2) - 1
\end{aligned}$$

A discrete Fourier ansatz

$$u_{k_1, k_2}(x_1, x_2) = \exp\left(\frac{2\pi i}{N}(k_1 x_1 + k_2 x_2)\right)$$

yields the same eigenvalues. Setting  $k_1 = k_2 = 0$ , we verify that the maximal eigenvalue of  $A$  is always equal to the number of neighbors.

Assuming a large lattice size  $N$ , the minimal eigenvalues are determined by differentiating with respect to  $\phi_i$ . For the range of eigenvalues  $\lambda$  of  $V^{-1}A$  we finally obtain:

$$\begin{aligned}
v.N.1 : \quad & -1 \leq \lambda_k \leq 1 \\
M.1 : \quad & -\frac{1}{2} \leq \lambda_k \leq 1 \\
v.N.2 : \quad & -\frac{13}{36} \leq \lambda_k \leq 1 \\
M.2 : \quad & -\frac{29}{96} < \lambda_k \leq 1 .
\end{aligned}$$

(In general, the lower bound given in these expressions refers to the continuous limit  $N \rightarrow \infty$  of  $\phi$  and is only approximately realized for discrete  $\phi$ , i.e. finite  $N$ .) For the case of global coupling one finds  $-\frac{1}{N^2-1} \leq \lambda \leq 1$  and, in the limit  $N \rightarrow \infty$ ,  $0 \leq \lambda \leq 1$ .

The spectrum of a regular graph can be similarly obtained for higher dimensions as well as for other lattice types. As an example we mention a triangular lattice (six nearest neighbors) which can be considered as a square lattice with the diagonals in one direction added. The adjacency matrix is given by

$$A_{\text{triangle}} = P_1 + P_1^{-1} + P_2 + P_2^{-1} + P_1 P_2 + P_1^{-1} P_2^{-1} ,$$

and the corresponding eigenvalues of  $V^{-1}A$  are:

$$\lambda_{k_1, k_2} = \frac{1}{6} (2 \cos \phi_1 + 2 \cos \phi_2 + 2 \cos(\phi_1 + \phi_2)) .$$

The maximal eigenvalue is  $\lambda_{\max} = +1$  and the minimal eigenvalue is  $\lambda_{\min} = -\frac{1}{2}$ . This is identical to the case of a square lattice with a 1st order Moore neighborhood.

### 3 Stability Analysis for Constant Solutions with Synchronous Updating

Now we consider the stability of a constant solution,

$$\bar{u}(n, x) \equiv \bar{u} \quad \text{for all } n, x ,$$

of a CML (eq. 1). Given our normalization of parameters, an example of such a constant solution is the critical point of the logistic map:  $\bar{u} = \frac{r-1}{r}$ . (As will be shown in Sec. 3.3, this is – apart from  $\bar{u} = 0$  – the only constant solution if  $\gamma = 0$ .) Furthermore, we consider a synchronous update of the lattice, which strictly corresponds to eq. (1). Special features related to asynchronous updating will be discussed in section 4.

Let  $\{u_k(x)\}$  be a complete set of solutions of the eigenvalue equation for the normalized adjacency matrix  $V^{-1}A$ :

$$\sum_y (V^{-1}A)(x, y) u_k(y) = \frac{1}{n_x} \sum_{y \sim x} u_k(y) = \lambda^k u_k(x) .$$

For the stability analysis we consider fluctuations around the constant solution,

$$u_n(x) = \bar{u} + \delta a_n^k u_k(x) ,$$

and obtain:

$$\delta a_{n+1}^k = (1 - \epsilon) f'(\bar{u}) \delta a_n^k + \epsilon \lambda_k g'(\bar{u}) \delta a_n^k . \quad (3)$$

Hence, the constant solution is stable if  $\epsilon$  satisfies the following inequalities:

$$-1 < (1 - \epsilon) f'(\bar{u}) + \epsilon \lambda_k g'(\bar{u}) < +1 \quad \text{for all } k . \quad (4)$$

Inserting the logistic map for  $f$ , and using  $g$  as defined in eq. (2) we find:

$$f'(\bar{u}) = 2 - r \quad \text{and} \quad g'(\bar{u}) = \alpha - (r - 2)\beta + (r - 2)^2\gamma .$$

This leads to the stability conditions:

$$r - 3 < \epsilon (r - 2 + \lambda_k [\alpha - (r - 2)\beta + (r - 2)^2\gamma]) < r - 1 \quad \text{for all } k . \quad (5)$$

Note that  $\alpha - (r - 2)\beta + (r - 2)^2\gamma$  can be positive or negative. Depending on this sign, it is the smallest or the largest eigenvalue  $\lambda_k$  of the normalized adjacency matrix for which one of the inequality conditions in eq. (5) is first violated.

Due to the many parameters ( $\alpha$ ,  $\beta$ ,  $\gamma$ ,  $\epsilon$  and  $r$ ) in the CML (eq. 1), and in the stability conditions (eq. 5), we restrict our discussion to special cases emphasizing those parameter ranges which have been numerically investigated in previous work.

### 3.1 Pure Causal Coupling

Pure causal coupling is characterized by  $\beta = \gamma = 0$  and  $\alpha = 1$ . The stability conditions (eq. 5) then read:

$$r - 3 < \epsilon(r - 2 + \lambda_k) < r - 1 .$$

The lower inequality defines the critical coupling strength:

$$\epsilon_c = \frac{r - 3}{r - 2 + \lambda_{\min}} . \quad (6)$$

Inserting the different minimal eigenvalues for the various neighborhoods we find:

$$\begin{aligned} \text{v. N. 1} \quad \epsilon_c &= \frac{r - 3}{r - 2 - 1} = 1 \\ \text{M. 1} \quad \epsilon_c &= \frac{r - 3}{r - 2.5} \\ \text{v. N. 2} \quad \epsilon_c &= \frac{r - 3}{r - 2 - \frac{13}{36}} = \frac{r - 3}{r - 2.361\dots} \\ \text{M. 2} \quad \epsilon_c &= \frac{r - 3}{r - 2 - \frac{29}{96}} = \frac{r - 3}{r - 2.302\dots} \\ \text{global} \quad \epsilon_c &= \frac{r - 3}{r - 2} . \end{aligned}$$

These results can be compared with numerical simulations presented in [9]. Figure 1 gives a compact representation of those results, showing the critical coupling strength  $\epsilon_c$ , beyond which the unstable fixed point of  $u$  is stabilized, as a function of the control parameter  $r$  of the logistic map for different neighborhoods as indicated in the figure and for synchronous updating. The case of global coupling turns out to be realized for asynchronous updating (cf. Sec. 4) as well.

Note that for the first order von Neumann neighborhood the constant solution is always unstable for  $\epsilon < 1$ . For  $r = 4$  (right hand side of Fig. 1) we obtain the following critical values of  $\epsilon$ :

$$\begin{aligned} \text{v. N. 1} \quad \epsilon_c &= 1 \\ \text{M. 1} \quad \epsilon_c &= 0.66\dots \\ \text{v. N. 2} \quad \epsilon_c &= 0.61\dots \\ \text{M. 2} \quad \epsilon_c &= \frac{96}{163} = 0.589\dots \\ \text{global} \quad \epsilon_c &= 0.5 . \end{aligned}$$

It is easy to check that the numerical results of Fig. 1 agree perfectly well with the theoretical results according to eq. (6).



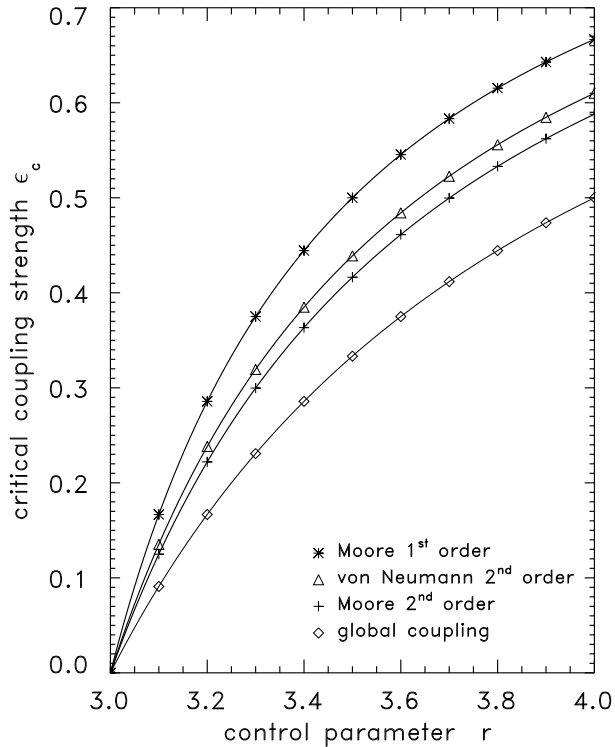


Figure 1: Critical coupling strength for stabilization onset,  $\epsilon_c$ , as a function of  $r$ ,  $3 \leq r \leq 4$ . The individual values are numerical results for synchronous updating. All curves are given by the functions of  $\epsilon_c$  on  $r$  according to eq. (6).

### 3.2 Causal and Non-Causal Coupling

Next we consider the case  $\gamma = 0$ ,  $\beta = 1 - \alpha$ , and  $r = 4$ . This situation has been investigated numerically in [5]. From eq. (5), we now obtain the stability conditions:

$$1 < \epsilon(2 + \lambda_k(3\alpha - 2)) < 3. \quad (7)$$

For  $\alpha = \frac{2}{3}$ , this becomes independent of the neighborhood. In this case the critical value  $\epsilon_c$  derived from the lower bound of eq. (7) is:

$$\epsilon_c(\alpha = \frac{2}{3}) = \frac{1}{2}.$$

For  $\alpha > \frac{2}{3}$ , the minimal eigenvalue of the adjacency matrix determines the stability of the CML with respect to the lower bound in eq. (7) and we find:

$$\begin{aligned} \text{v. N. 1} \quad \epsilon_c &= \frac{1}{4 - 3\alpha} \\ \text{M. 1} \quad \epsilon_c &= \frac{1}{3 - \frac{3}{2}\alpha} \end{aligned}$$

$$\begin{aligned}
\text{v. N. 2} \quad \epsilon_c &= \frac{36}{98 - 39\alpha} \\
\text{M. 2} \quad \epsilon_c &= \frac{96}{250 - 87\alpha} \\
\text{global} \quad \epsilon_c &= \frac{1}{2} .
\end{aligned}$$

For  $\alpha < \frac{2}{3}$ , the lower bound is first saturated for the maximal eigenvalue  $\lambda_{\max} = 1$  of the normalized adjacency matrix. Since this is independent of the neighborhood and holds for any simple graph, we have the result:

$$\epsilon_c = \frac{1}{3\alpha} .$$

As  $\epsilon \leq 1$  there is no critical value for  $\epsilon$  for  $\alpha < \frac{1}{3}$ . In this regime the constant solution is generally unstable (for synchronous updating).

Figure 2 shows the numerical results for combinations of causal and non-causal coupling for both synchronous and asynchronous updating. All results for synchronous updating agree perfectly with our theoretical results. Asynchronous updating will be discussed separately in Sec. 4.

### 3.3 Causal, Non-Causal, and Anti-Causal Coupling

This case may be of less practical interest but can shed some light on general features of CMLs. In particular, it presents features which are not shared by the coupling scenarios discussed in the preceding sections. We distinguish three cases: pure anti-causal coupling ( $\gamma = 1, \alpha = \beta = 0$ ), combinations of causal and anti-causal coupling ( $\beta = 0, \alpha = 1 - \gamma$ ), and combinations of non-causal and anti-causal coupling ( $\alpha = 0, \beta = 1 - \gamma$ ). Our discussion refers mostly to the stability of the constant solution at  $\bar{u} = \frac{r-1}{r}$ . For  $\gamma \neq 0$  there are additional constant solutions which depend on  $\epsilon$ .

#### 3.3.1 Pure Anti-Causal Coupling: $\gamma = 1, \alpha = \beta = 0$

The stability conditions in this case are given by:

$$r - 3 < \epsilon (r - 2 + \lambda_k(r - 2)^2) < r - 1 .$$

For the lower bound, we only obtain solutions in the range  $0 \leq \epsilon \leq 1$  if:

$$\lambda_{\min} > -\frac{1}{(r - 2)^2} . \tag{8}$$

For  $r = 4$ , this condition is not fulfilled for the neighborhoods considered in this paper except for global coupling.

For a given graph, eq. (8) is satisfied if

$$r \leq 2 + \sqrt{\frac{1}{|\lambda_{\min}|}} .$$

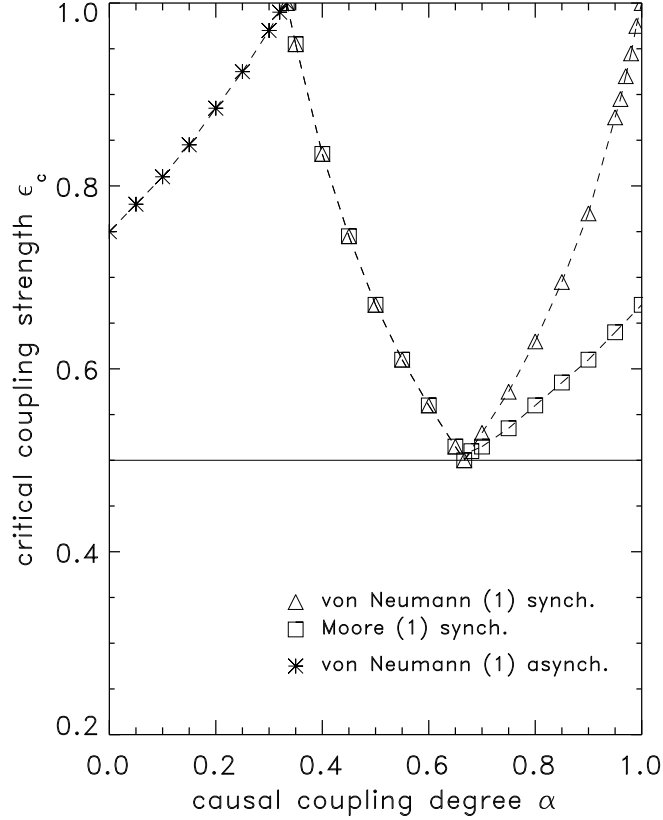


Figure 2: Critical coupling strength  $\epsilon_c$  for stabilization onset as a function of the degree  $\alpha$  of causal coupling for  $r = 4$ . Different symbols refer to different neighborhoods as explained in the figure. The solid line at  $\epsilon_c = 0.5$  characterizes the situation for asynchronous updating, independent of the neighborhood considered.

In this case, the stability conditions are given by

$$\frac{r-3}{(r-2) - |\lambda_{\min}|(r-2)^2} < \epsilon < \frac{r-1}{(r-2) + (r-2)^2}.$$

### 3.3.2 Causal and Anti-Causal Coupling: $\beta = 0$ , $\alpha = 1 - \gamma$

For  $r = 4$ , the stability conditions now assume the form:

$$1 < \epsilon(2 + \lambda_k(1 + 3\gamma)) < 3.$$

There is a general upper bound

$$\epsilon < \frac{1}{1 + \gamma},$$

beyond which the constant solution at the unstable fixed point remains unstable. The lower bound for  $\epsilon$  depends on the type of neighborhood:

v. N. 1	$\epsilon > \frac{1}{1 - 3\gamma}$	nowhere satisfied
M. 1	$\epsilon > \frac{2}{3 - 3\gamma}$	if $\gamma < \frac{1}{3}$
v. N. 2	$\epsilon > \frac{36}{59 - 39\gamma}$	if $\gamma < \frac{23}{39}$
M. 2	$\epsilon > \frac{96}{163 - 87\gamma}$	if $\gamma < \frac{67}{87}$
global	$\epsilon > \frac{1}{2}$	for all $\gamma$ .

Fig. 3 shows numerically obtained CML state values as a function of coupling strength  $\epsilon$  for selected values of  $\gamma$  and for a first order von Neumann neighborhood. There is no stable solution at the unstable fixed point, corresponding to our theoretical result that the stability condition is nowhere satisfied in this case. However, we observe  $\epsilon$ -dependent solutions different from the unstable fixed point. This is due to the fact that for constant solutions and  $\gamma \neq 0$  eq. (1) is of fourth order. The solutions can be characterized (for  $r = 4$ ) by

$$\bar{u}_{1/2} = \frac{5}{8} \pm \frac{1}{8} \sqrt{5 - \frac{4(1 - \epsilon)}{\epsilon\gamma}}. \quad (9)$$

Real solutions exist only for  $\epsilon \geq \frac{4}{4+5\gamma}$  as can be recognized by the stable regimes in Fig. 3b-e. In Fig. 3a there is only a bistable solution.

### 3.3.3 Non-Causal and Anti-Causal Coupling: $\alpha = 0$ , $\beta = 1 - \gamma$

For several interesting values of  $\gamma$ , Fig. 4 shows numerically obtained state values of the CML as a function of coupling strength  $\epsilon$  for a first order von Neumann neighborhood, Fig. 5 shows the same for a first order Moore neighborhood.

The stability conditions for  $r = 4$  read:

$$1 < \epsilon(2 + \lambda_k(6\gamma - 2)) < 3.$$

For  $\gamma = \frac{1}{3}$ , we find  $\epsilon_c = \frac{1}{2}$  from the lower bound, while the upper bound gives no restriction. For  $\frac{1}{6} < \gamma < \frac{1}{3}$ , only the maximal eigenvalue is relevant and the conditions are independent of the considered graph. We find:

$$\epsilon > \frac{1}{6\gamma}.$$

This is confirmed by the numerical results for a first order von Neumann neighborhood in Fig. 4b-e and for a first order Moore neighborhood in Fig. 5e.

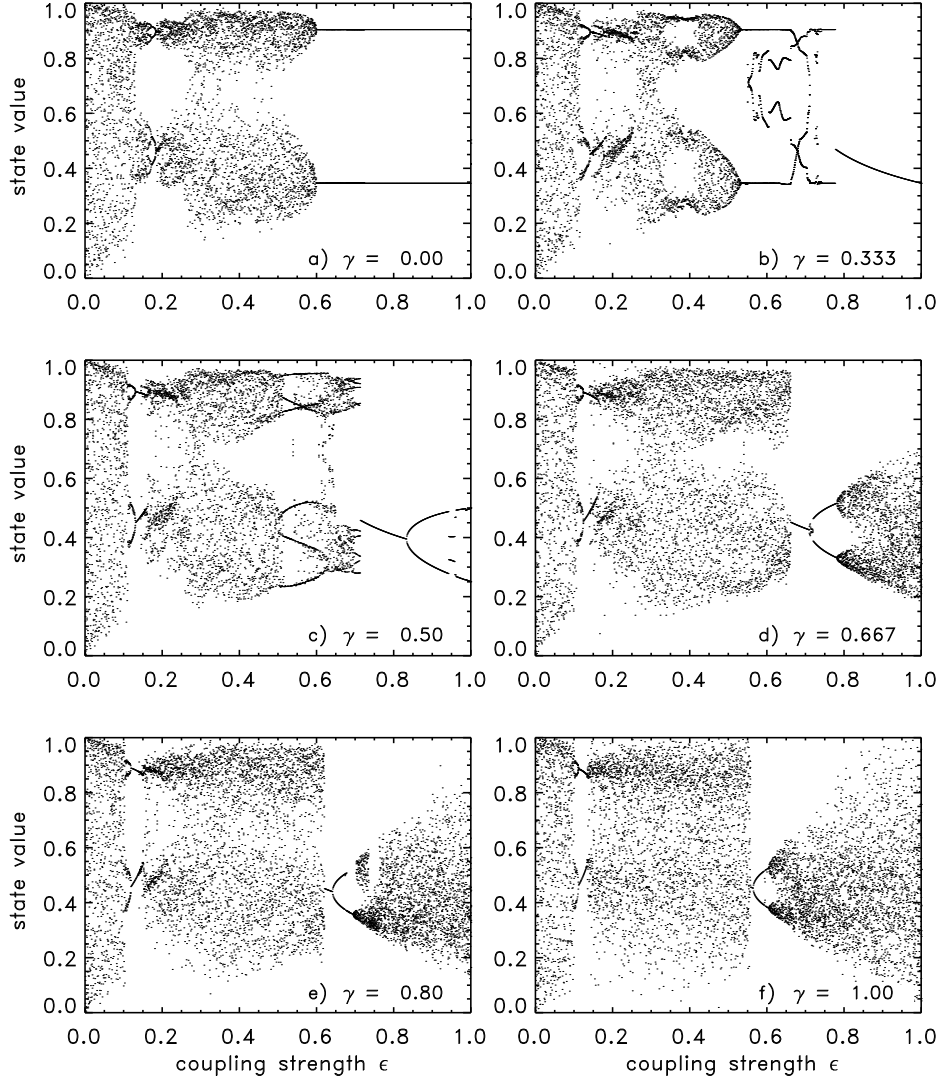


Figure 3: Stability diagram for synchronously updated CMLs with a von Neumann neighborhood of order 1. For selected values of  $\gamma = 1 - \alpha$ , the distribution of states is plotted versus coupling strength  $\epsilon$ . Simulations are based on random initial conditions on a  $50 \times 50$  lattice, at least 5000 iterations, and  $r = 4$ .

There is no stability for  $\gamma < \frac{1}{6}$ . (The upper bound leads to no restriction.) This can be seen in Fig. 4e-f for a first order von Neumann neighborhood and in Fig. 5f for a first order Moore neighborhood.

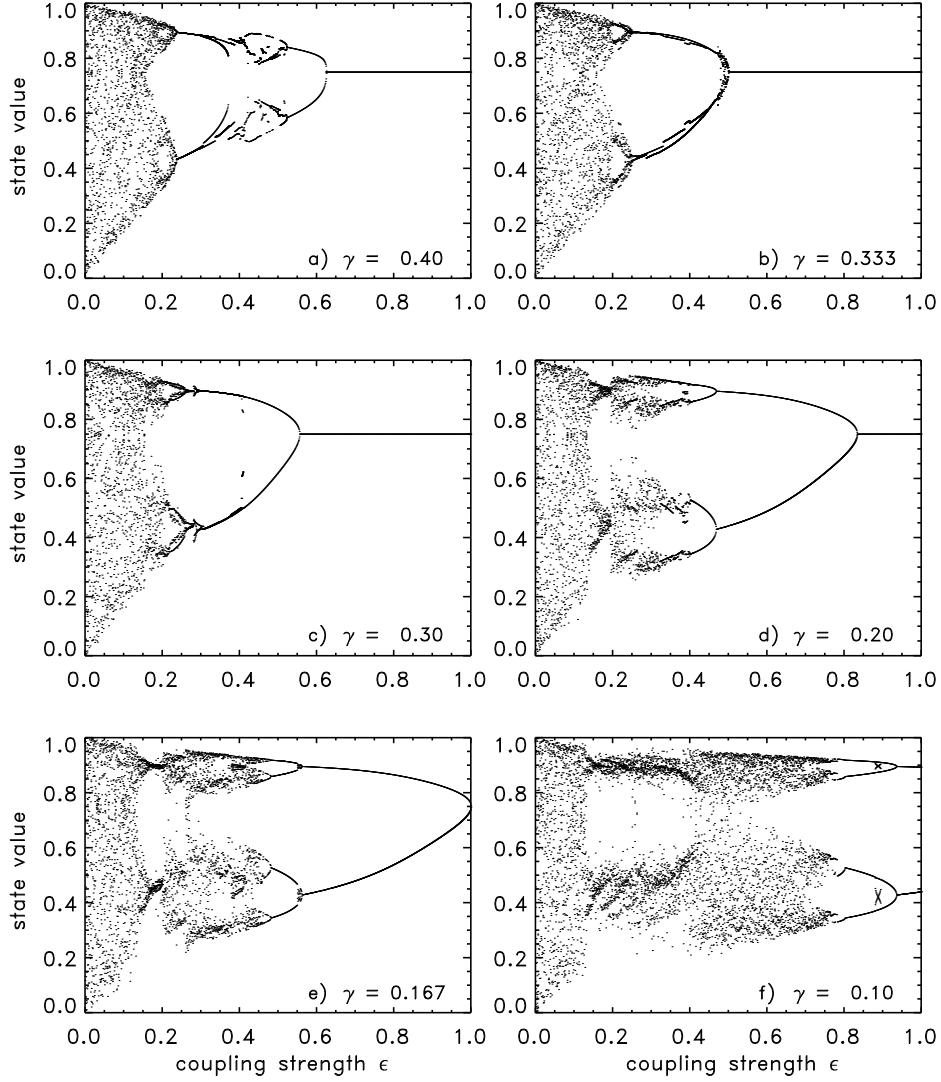


Figure 4: Stability diagram for synchronously updated CMLs with a von Neumann neighborhood of order 1. For selected values of  $\gamma = 1 - \beta$ , the distribution of states is plotted versus coupling strength  $\epsilon$ . Simulation details are as in Fig. 3.

For  $\gamma > \frac{1}{3}$  we find:

v. N. 1	$\frac{1}{4 - 6\gamma} < \epsilon$	if	$\frac{1}{3} < \gamma < \frac{1}{2}$
M. 1	$\frac{1}{3 - 3\gamma} < \epsilon < \frac{1}{2\gamma}$	if	$\frac{1}{3} < \gamma < \frac{3}{5}$
v. N. 2	$\frac{18}{49 - 39\gamma} < \epsilon < \frac{1}{2\gamma}$	if	$\frac{1}{3} < \gamma < \frac{49}{75}$
M. 2	$\frac{48}{125 - 87\gamma} < \epsilon < \frac{1}{2\gamma}$	if	$\frac{1}{3} < \gamma < \frac{125}{183}$
global	$\frac{1}{2} < \epsilon < \frac{1}{2\gamma}$	for all	$\gamma$ .

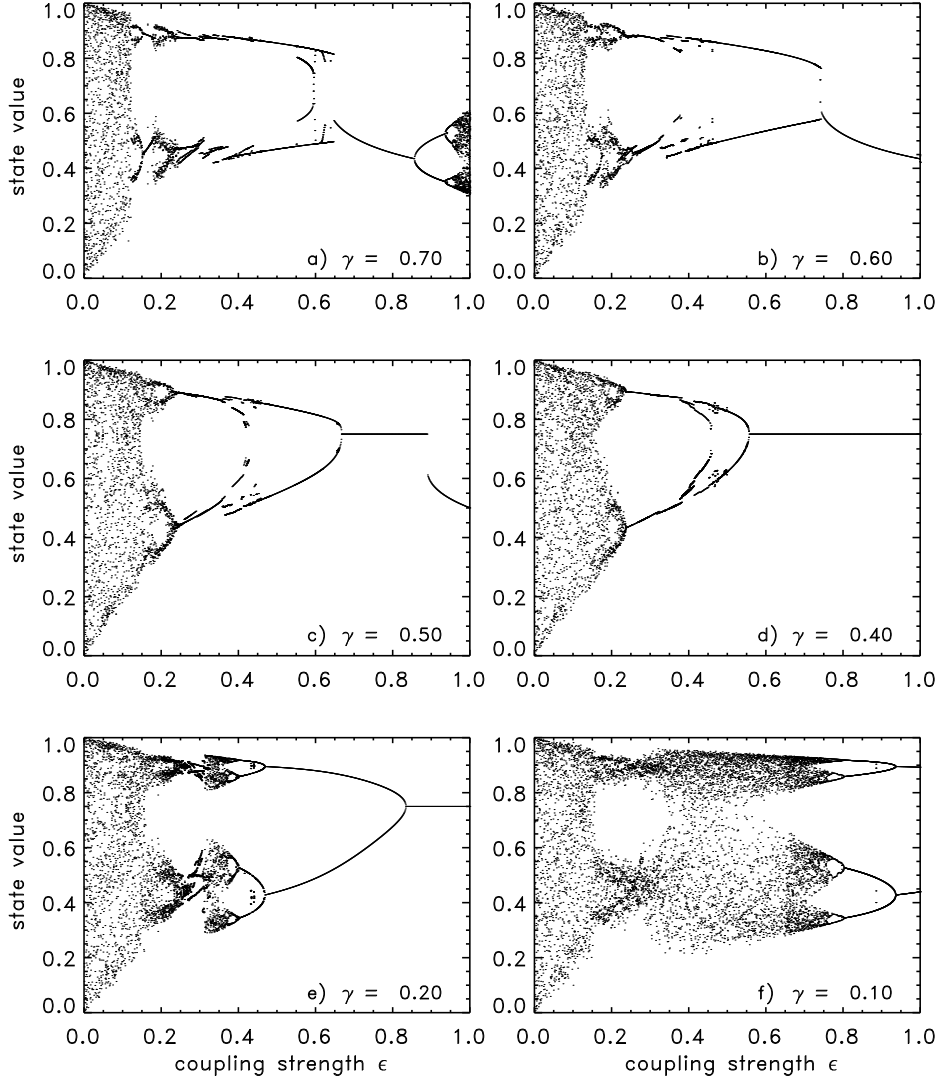


Figure 5: Stability diagram for synchronously updated CMLs with a Moore neighborhood of order 1. For selected values of  $\gamma = 1 - \beta$ , the distribution of states is plotted versus coupling strength  $\epsilon$ . Simulation details are as in Fig. 3.

For the regime  $\frac{1}{6} < \gamma < \frac{1}{3}$ , the theoretical results are confirmed by the example in Fig. 4a for a first order von Neumann neighborhood and in Fig. 5d for a first order Moore neighborhood.

While a first order von Neumann neighborhood produces no stable solution for  $\gamma \geq 0.5$ , this is different for a first order Moore neighborhood (and for higher order neighborhoods). Figure 5c shows  $\epsilon_c = 0.67$  at  $\gamma = 0.5$  for a first order Moore neighborhood. In addition to the theoretically predicted stability of the unstable fixed point for all  $\epsilon_c < 1$ , anti-causal coupling ( $\gamma \neq 0$ ) yields  $\epsilon$ -dependent stable

solutions as well. For  $r = 4$  they are now given by

$$\bar{u}_{1/2} = \frac{5}{8} \pm \frac{1}{8} \sqrt{9 - \frac{4}{\epsilon\gamma}}. \quad (10)$$

Real solutions exist only for  $\epsilon \geq \frac{4}{9\gamma}$  and can be recognized in Fig. 5a-c. In particular, Fig. 5c shows a discontinuous transition of the constant solution from  $\bar{u} = \frac{r-1}{r} = \frac{3}{4}$  to  $\bar{u} = \frac{5}{8}$  at  $\epsilon = \frac{8}{9}$ , which represents a second critical coupling value at  $\gamma = 0.5$  in Fig. 6.

The constant solution for a first order Moore neighborhood becomes unstable when  $\gamma > \frac{1}{2}$  and  $\epsilon < \frac{1}{2\gamma}$ . This is confirmed in Fig. 5a-b. Upper and lower bounds coincide for  $\gamma = 0.6$ .

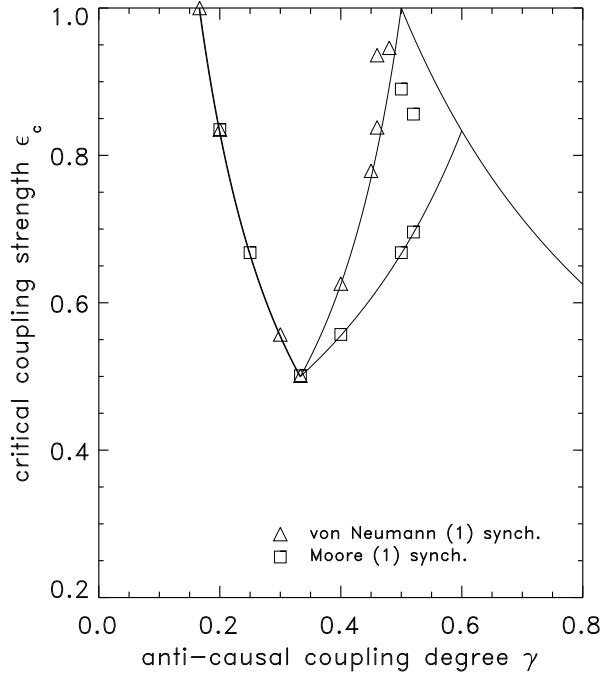


Figure 6: Critical coupling strength  $\epsilon_c$  for stabilization onset as a function of the degree  $\gamma = 1 - \beta$  of anti-causal versus non-causal coupling for  $r = 4$  and for synchronous updating. The solid lines represent theoretical predictions and the dots refer to numerically obtained values for von Neumann and Moore neighborhoods of first order.

All results for combinations of non-causal and anti-causal coupling with synchronous update for first order neighborhoods are compactly summarized in Figure 6, representing  $\epsilon_c$  as a function of  $\gamma = 1 - \beta$  (for  $r = 4$ ). Most numerical data and theoretical curves agree perfectly. Results around  $\gamma = 0.5$ , deviating from the curves in Fig. 6, do still satisfy the stability inequalities. Possible reasons for these deviations are due to coexisting stable solutions. This is presently under investigation.



## 4 Asynchronous Updating

Our results so far were derived for a synchronous updating scenario for the CML configurations. For asynchronous updating the analytic treatment is more elaborate. The possibility of different types of asynchronous updates makes this even worse.

For synchronous updating, we can interpret the CML (eq. 1) as the iteration of a single mapping  $F$  which maps a vector  $\{u(n, x)\}$  (with components  $x$ ) to a vector  $\{u(n+1, x)\}$ :

$$F : \{u(n, x)\} \longrightarrow \{u(n+1, x)\}$$

where  $u(n+1, x)$  is given by eq. (1) for all  $x$  (i.e., synchronously). The linear approximation around the constant solution (leading to eq. 3) can be written as

$$\delta u_{n+1}(x) = \sum_y F'(x, y) \delta u_n(y)$$

where the matrix  $F'(x, y)$  is given by:

$$F'(x, y) = (1 - \epsilon) f'(\bar{u}) \delta(x, y) + \epsilon g'(\bar{u}) (V^{-1} A)(x, y)$$

with  $\delta(x, y)$  as Kronecker's  $\delta$ . The stability condition (eq. 4) is simply a condition for the eigenvalues of  $F'$ .

By contrast, asynchronous updating corresponds to a set of mappings (one for each vertex  $z$ ) such that:

$$F_z : \{u(n, x)\} \longrightarrow \{u(n+1, x)\} ,$$

where now  $\{u(n+1, x)\}$  is given by:

$$u(n+1, x) = \begin{cases} u(n, x) & \text{for } x \neq z \\ (1 - \epsilon) f(u(n, x)) + \frac{\epsilon}{n_x} \sum_{y \sim x} g(u(n, x)) & \text{for } x = z \end{cases} .$$

Correspondingly, the linear approximation now depends on the vertex  $z$ , for which the update has been made:

$$F'_z(x, y) = \begin{cases} \delta(x, y) & \text{for } x \neq z \\ F'(x, y) & \text{for } x = z \end{cases} .$$

The stability condition is now a condition for the eigenvalues of a matrix, which is a product of  $F'_z$ -matrices, where the product runs over  $z$  either randomly or according to some specific sequential rule. In general, the matrices  $F'_z(x, y)$  do not commute for different values of  $z$  which makes it difficult to determine the eigenvalues of this product.

However, despite this difficulty to derive an exact analytical solution for the stability of asynchronously updated configurations, there is an intuitive argument for the stability of such configurations.

Consider some perturbation  $\delta u(x)$  around a constant solution  $\bar{u}$  of the CML. The lower bound of the stability equation (eq. 4) corresponds to a change of  $\delta u(x)$ , including a change in sign, at the vertex  $x$  where the update is made. In particular, a perturbation proportional to the eigenfunction of the adjacency matrix for which the corresponding eigenvalue violates the lower stability bound for the constant solution is simply multiplied by  $-1$  at the critical value of  $\epsilon$ .

When an update is made at some vertex  $z$ , we can assume that its neighbors have been randomly updated before and therefore their signs have changed randomly. This implies that, on average, the neighbors of vertex  $z$  cancel and do not contribute to the update, so we have an effective update equation of the form:

$$\delta u(n+1, z) = (1 - \epsilon) f'(\bar{u}) \delta u(n, z) .$$

The lower bound of the stability condition of this equation reads:

$$-1 < (1 - \epsilon) f'(\bar{u}) ,$$

which for the logistic mapping becomes:

$$\epsilon > \frac{r-3}{r-2} .$$

This equation has been derived from different arguments in [9]. It corresponds to the solid curve shown in Fig. 1.

However, if  $\epsilon$  approaches the upper bound of the stability inequality, a perturbation  $\delta u(x)$  does not change its sign. Therefore, even if a random number of neighbors of a vertex  $z$ , which is to be updated, have already been updated before, their fluctuations will not necessarily cancel on average. This situation is similar to synchronous updating. This argument makes it plausible that the upper bound for  $\epsilon$ , as derived from synchronous updating, is also valid for asynchronous updating.

Among the various situations studied numerically in [5, 9], there is only one case where the upper bound of the stability inequality becomes relevant: combinations of causal and non-causal coupling in the regime  $\alpha < \frac{1}{3}$  for a first order von Neumann neighborhood. For this case the upper bound stability condition (7) reads:

$$\epsilon < \frac{3}{4 - 3\alpha} .$$

This has been numerically confirmed for a number of examples shown in Fig. 2.

## 5 Generalized Neighborhoods

In the preceding sections, all neighbors of a vertex have been treated identically. However, it is possible to consider more general, inhomogeneous couplings of the vertices of the graph on which the CML is defined. For instance, the coupling strength may depend on the distance on the graph (where distance refers to the

length of the minimal path). Such generalized couplings are also suggested by renormalization methods, which, even if the starting point is a nearest neighbor coupling, effectively lead to couplings between more distant points.

The most general case is given by a symmetric adjacency matrix with a non-negative coupling between any two vertices:

$$A^{(g)}(x, y) = A^{(g)}(y, x) \geq 0 \quad A^{(g)}(x, x) = 0 .$$

We can define the generalized valence matrix by:

$$V^{(g)}(x, y) = \begin{cases} \sum_z A^{(g)}(x, z) & \text{for } x = y \\ 0 & \text{otherwise} \end{cases} ,$$

and we assume that  $V^{(g)}(x, x) > 0$  for all  $x$ . As in Sec. 2, one can show that  $(\mathbf{1} \pm V^{(g)-1}A^{(g)})$  is non-negative and that the largest eigenvalue of  $V^{(g)-1}A^{(g)}$  is +1 (corresponding to the constant function on the graph). In the context of Markov processes the matrix  $V^{(g)-1}A^{(g)}$  is called a Markov matrix.

A simple example is given by a mixture of von Neumann and Moore neighborhoods of first order, where nearest horizontal and vertical neighbors are linked by a coupling  $a_1$  and the additional diagonal neighbors are linked by a coupling  $a_2$ . We now define the generalized adjacency matrix

$$A(x, y) = \begin{cases} a_1 & \text{if } x \text{ and } y \text{ are nearest neighbors} \\ a_2 & \text{if } x \text{ and } y \text{ are diagonal neighbors} \\ 0 & \text{otherwise} \end{cases} .$$

This matrix can be written in the form:

$$A(x, y) = a_1(P_1 + P_1^{-1} + P_2 + P_2^{-2}) + a_2(P_1P_2 + P_1P_2^{-1} + P_1^{-1}P_2 + P_1^{-1}P_2^{-1}) ,$$

and the corresponding eigenvalues  $\hat{\lambda}$  of  $A$  are:

$$\hat{\lambda} = 2a_1(\cos \phi_1 + \cos \phi_2) + 4a_2 \cos \phi_1 \cos \phi_2 .$$

The maximal eigenvalue (equal to the generalized valence of a vertex) and the minimal eigenvalue of  $A$  are:

$$\hat{\lambda}_{\max} = v = 4(a_1 + a_2) \quad \text{and} \quad \hat{\lambda}_{\min} = -4\max(a_1, a_2) .$$

The normalized minimal eigenvalue can now be tuned between the case of first order von Neumann ( $\lambda_{\min} = -1$ ) for  $a_2 = 0$  (equivalently,  $a_1 = 0$ ) and first order Moore ( $\lambda_{\min} = -\frac{1}{2}$ ) for  $a_1 = a_2$ .

An interesting case occurs if the coupling  $a(L)$  depends only on the lattice-distance  $L$  between two points such that  $a(L_1 + L_2) = a(L_1)a(L_2)$ . In this case  $a(L) = p^L$  for some positive constant  $p$  which we assume to be smaller than 1 in order to avoid divergencies on infinite lattices. For the following we assume the

lattice to be rectangular,  $d$ -dimensional and consider the limit of infinite lattice size,  $N \rightarrow \infty$ . The adjacency matrix can then be written in the form:

$$A = \prod_{i=1}^d \left( \mathbf{1} + \sum_{L=1}^{\infty} p^L (P_i^L + P_i^{-L}) \right) - \mathbf{1}$$

with eigenvalues:

$$\lambda = \prod_{i=1}^d \left( 1 + 2 \sum_{L=1}^{\infty} p^L \cos L\phi_i \right) - 1 = \prod_{i=1}^d \left( \frac{1 - p^2}{1 - 2p \cos \phi_i + p^2} \right) - 1 .$$

For the maximal and minimal normalized eigenvalues we finally obtain:

$$\lambda_{\max} = 1 \quad \lambda_{\min} = - \left( \frac{1 - p}{1 + p} \right)^d .$$

The significance of this exercise is obvious. Already for the 1-dimensional lattice (the circular graph) we can mimick, by a suitable tuning of  $p$ , the largest and smallest eigenvalues of any other arbitrary graph or generalized coupling. These eigenvalues are independent of the functions  $f(x)$  (for which we used the logistic map) and  $g(x)$ . The stability of the constant solution of a CML does not depend on any other property of the graph except these two eigenvalues.

## 6 Summary

Coupled map lattices (CMLs) and other complex model systems produce an overwhelming phenomenological variety of features which are notoriously difficult to classify and explain in a compact and comprehensive way. A promising concept for such purposes is the concept of stability since it characterizes complex systems in their different dynamical regimes in a most basic fashion.

The stability of CMLs has been studied numerically by a number of authors before. A large class of such studies were carried out in the context of synchronizing and controlling complex systems. In contrast, analytical tools explaining the numerical results have not been broadly applied so far. Insofar as CMLs can be considered as implemented on special types of graphs, spectral graph theory provides a particularly convenient option to analyze the stability of CMLs theoretically. The maximal and minimal eigenvalues of the normalized adjacency matrix of the graph, on which the CML is defined, determine its stability properties.

We used these tools to analyze the stability properties of CMLs for different types of neighborhoods, different coupling scenarios and for different updating rules. In this paper we focused on the stability at or around temporally constant solutions of the CML as a whole. Particularly interesting is the case of globally stable solutions at locally unstable fixed points, which are independent of the coupling strength  $\epsilon$ . In addition we discovered constant solutions which are explicitly  $\epsilon$ -dependent.

For synchronous updating of the CML, we derived exact stability conditions for causal, non-causal, and anti-causal coupling. These different coupling scenarios distinguish whether states of a vertex of the graph are assumed to interact with their preceding, simultaneous, or future neighboring states, respectively. The considered neighborhoods are of low-order von Neumann and Moore type. All theoretical results agree excellently with numerical studies published earlier. Novel numerical simulations, referring to situations not treated before, additionally confirm our theoretical results.

For asynchronous updating, the stability analysis is in general more involved than for synchronous updating. In the case of a random updating sequence, the derivation simplifies and, again, gives results that agree with those of earlier numerical studies. A heuristic stability condition derived earlier could be confirmed as well.

Finally, we generalized our approach to inhomogeneous neighborhoods, such as mixtures of neighborhoods of different types or coupling strengths depending on the distance from a vertex. It could be shown that the stability of constant solutions of CMLs is completely characterized by the maximal and minimal eigenvalues of its normalized adjacency matrix, independent of the dynamics of the vertices and independent of the causality features assumed for coupling.

## Acknowledgments

We are grateful to one of the referees for several detailed and helpful suggestions and corrections concerning the first version of the manuscript.

## References

- [1] A. Turing. The chemical basis of morphogenesis. *Transactions of the Royal Society London, Series B* **237**, 37–72 (1952).
- [2] K. Kaneko, ed. *Theory and Applications of Coupled Map Lattices*. Wiley, New York, 1993.
- [3] A. Kuhn, A. Aertsen, and S. Rotter. Neuronal integration of synaptic input in the fluctuation-driven regime. *Journal of Neuroscience* **24**, 2345–2356 (2004).
- [4] M. Mehta and S. Sinha. Asynchronous updating of coupled maps leads to synchronization. *CHAOS* **10**, 350–358 (2000).
- [5] H. Atmanspacher and H. Scheingraber. Stabilization of causally and non-causally coupled map lattices. *Physica A* **345**, 435–447 (2005).
- [6] C. Masoller, A.C. Marti, and D.H. Zanette. Synchronization in an array of globally coupled maps with delayed interactions. *Physica A* **325**, 186–191 (2003).
- [7] C. Li, S. Li, X. Liao, and J. Yu. Synchronization in coupled map lattices with small-world delayed interactions. *Physica A* **335**, 365–370 (2004).

- [8] F. Atay, J. Jost, and A. Wende. Delays, connection topology, and synchronization of coupled chaotic maps. *Physical Review Letters* **92**, 144101 (2004).
- [9] H. Atmanspacher and H. Scheingraber. Inherent global stabilization of unstable local behavior in coupled map lattices. *Int. Journal of Bifurcation and Chaos*, in press (2005). lanl preprints nlin.CD/0407008.
- [10] H. Atmanspacher, T. Filk, and H. Scheingraber. The significance of causally coupled, stable neuronal assemblies for the psychological time arrow. Submitted.
- [11] K. Kaneko and I. Tsuda. *Complex Systems: Chaos and Beyond*. Springer, Berlin, 2000.
- [12] E.D. Lumer and G. Nicolis. Synchronous versus asynchronous dynamics in spatially distributed systems. *Physica D* **71**, 440–452 (1994).
- [13] P. Marcq, H. Chaté, and P. Manneville. Universality in Ising-like phase transitions of lattices of coupled chaotic maps. *Physical Review E* **55**, 2606–2627 (1997).
- [14] J. Rolf, T. Bohr, and M.H. Jensen. Directed percolation universality in asynchronous evolution of spatiotemporal intermittency. *Physical Review E* **57**, R2503–R2506 (1998).
- [15] E. Ott, C. Grebogi, and J.A. Yorke. Controlling chaos. *Physical Review Letters* **64**, 1196–1199 (1990).
- [16] M. Mackey and J. Milton. Asymptotic stability of densities in coupled map lattices. *Physica D* **80**, 1–17 (1995).
- [17] J. Losson, J. Milton, and M.C. Mackey. Phase transitions in networks of chaotic elements with short and long range interactions. *Physica D* **81**, 177–203 (1995).
- [18] A. Lemaitre, H. Chaté, and P. Manneville. Cluster expansion for collective behavior in discrete-space dynamical systems. *Phys. Rev. Lett.* **77**, 486–489 (1996).
- [19] A. Lemaitre and H. Chaté. Nonperturbative renormalization group for chaotic coupled map lattices. *Phys. Rev. Lett.* **80**, 5528–5531 (1998).
- [20] V. Belykh, I. Belykh, N. Komrakov, and E. Mosekilde. Invariant manifolds and cluster synchronization in a family of locally coupled map lattices. *Discrete Dynamics* **4**, 245–256 (2000).
- [21] J. Jost and M.P. Joy. Spectral properties and synchronization in coupled map lattices. *Physical Review E* **65**, 016201 (2002).

- [22] V.N. Belykh, I.V. Belykh, and M. Hasler. Connection graph stability method for synchronized coupled chaotic systems. *Physica D* **195**, 159–187 (2004).
- [23] N. Biggs. *Algebraic Graph Theory*. Cambridge University Press, 1974.
- [24] D.M. Cvetković, M. Doob, and H. Sachs. *Spectra of Graphs*. Johann Ambrosius Barth, Heidelberg, 1995.
- [25] R.J. Wilson. *Introduction to Graph Theory*. Longman Scientific & Technical, Essex, 1985.